

# The pion and kaon electromagnetic form factors

J. Lowe

*Physics Department, University of New Mexico, Albuquerque, NM 87131*

M. D. Scadron

*Physics Department, University of Arizona, Tucson, AZ 85721*

## Abstract

We use recent data on  $K^+ \rightarrow \pi^+ e^+ e^-$ , together with known values for the pion form factor, to derive the kaon electromagnetic form factor for  $0 < q^2 < 0.125 \text{ (GeV/c)}^2$ . The results are then compared with predictions of the Linear  $\sigma$  Model, a quark-triangle model and Vector Meson Dominance. The first two models describe the data at least qualitatively, but the simple Vector Meson Dominance picture gives a detailed quantitative fit to the experimental results.

PACS numbers: 13.20.Eb and 13.25.Es

## 1. Introduction

The pion electromagnetic form factor,  $F_\pi(q^2)$ , is well studied experimentally. Many measurements, for both positive and negative  $q^2$ , have been reported in the literature [1]. Additional information comes from the pion charge radius, which is related to the slope of the form factor at  $q^2 = 0$  (see [2] for a summary of measurements of the pion charge radius). By contrast, much less is known for the kaon form factor,  $F_K(q^2)$ . There are some measurements [1] for negative  $q^2$ , but no data exist for  $q^2 > 0$ .

Information on  $F_K$  can be deduced indirectly from experimental data on the decay  $K^+ \rightarrow \pi^+ e^+ e^-$ , such as that provided by the recent high-statistics Brookhaven experiment E865 [3]. The amplitude for this decay was measured for  $q^2$  up to  $0.125 \text{ (GeV/c)}^2$ , the maximum allowed by the kinematics of this kaon decay. However, this amplitude does not give  $F_K$  directly, but rather the difference  $F_K(q^2) - F_\pi(q^2)$ . Since  $F_\pi(q^2)$  is relatively well known, then, this decay is a source of information on  $F_K$ .

The Linear Sigma Model ( $L\sigma M$ ) of Gell-Mann and Levy [4, 5, 6] has proved to be fruitful in describing low-energy properties of mesons. In a recent theoretical paper [5], the  $L\sigma M$ , and some related models, were used to study meson electromagnetic form factors. The authors restricted their comparison of  $F_\pi$  and  $F_K$  with experiment to a check of the slopes at  $q^2 = 0$ , using the measured pion and kaon charge radii. Here, we extend the comparison of these models with experiment, and we examine their success in reproducing  $F_K(q^2)$  for  $0 < q^2 < 0.125 \text{ (GeV/c)}^2$ .

In section 2, we extract the kaon form factor from the experimental data for  $K^+ \rightarrow \pi^+ e^+ e^-$ . In section 3, we derive both the pion and kaon form factors from the  $L\sigma M$ . In section 4, we introduce

the quark-triangle (QT) model and compare the QT predictions with experiment and in section 5, we give the Vector-Meson-Dominance (VMD) model predictions. In section 6, we examine the predictions of these models for the slopes of the form factors at  $q^2 = 0$ . Finally, section 7 summarises our results.

## 2. The decay $K^+ \rightarrow \pi^+ e^+ e^-$ and the kaon form factor

The decay  $K^+ \rightarrow \pi^+ e^+ e^-$  has been studied theoretically for many years. Already in 1985 it became clear [7] that the process is dominated by the “long-distance” (LD) terms, in which a virtual photon is radiated by either the pion or the kaon. However, it was not until the detailed data of experiment E865 [3] became available that a convincing description of both the scale and the  $q^2$  dependence of the amplitude was found [8].

Burkhardt *et al.* [8] considered four contributions to the amplitude, depicted in figure 1. The LD terms are those in figure 1(a) and (b). These two graphs are related to the pion and kaon form factors as shown below. Figure 1(c) represents all short-distance (SD) terms. These were already known in [7] to be small, and subsequent work [9] has shown them to be smaller than previously believed. Therefore here, as in ref. [8], we neglect the SD contribution from figure 1(c). Figure 1(d) is a “pion loop” term, first discussed by Ecker *et al.* [10]. Its contribution is small, but it gives a characteristic shape to the  $q^2$  dependence of the amplitude. As in [8], we take this term directly from [10]. Burkhardt *et al.* [8] gives a more detailed discussion of the contributions to the amplitude.

The pion and kaon form factors enter *via* the graphs of figure 1(a) and (b), which give the LD amplitude [8]

$$|A_{LD}(q^2)| = e^2 \left| \frac{\langle \pi^+ | H_W | K^+ \rangle}{m_{K^+}^2 - m_{\pi^+}^2} \right| \left| \frac{F_{\pi^+}(q^2) - F_{K^+}(q^2)}{q^2} \right|. \quad (1)$$

In the numerical calculations below, we take the value of the weak matrix element  $\langle \pi^+ | H_W | K^+ \rangle$  from [11]:

$$|\langle \pi^+ | H_W | K^+ \rangle| = (3.59 \pm 0.05) \times 10^{-8} \text{ GeV}^2.$$

Adding the pion loop amplitude, figure 1(d), from Ecker *et al.* [10], we obtain

$$\begin{aligned} A(q^2) &= A_{LD}(q^2) + A_{\pi loop}(q^2) \\ &= e^2 \left| \frac{\langle \pi^+ | H_W | K^+ \rangle}{m_{K^+}^2 - m_{\pi^+}^2} \right| \left| \frac{F_{\pi^+}(q^2) - F_{K^+}(q^2)}{q^2} \right| + A_{\pi loop}(q^2) \end{aligned} \quad (2)$$

from which

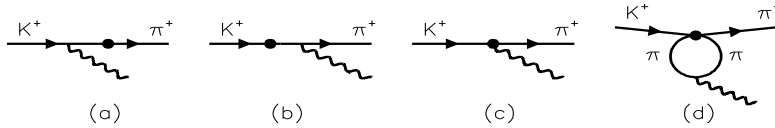


Figure 1: Graphs for  $K^+ \rightarrow \pi^+ e^+ e^-$ . (a) and (b) are long-distance graphs, (c) is a short-distance graph and (d) is the pion loop term. In each graph, the blob denotes the weak (strangeness-changing) vertex. The (off-shell) photon converts to  $e^+ e^-$ .

$$|F_K - F_\pi| = \frac{q^2(m_{K^+}^2 - m_{\pi^+}^2)}{e^2 |\langle \pi^+ | H_W | K^+ \rangle|} \left[ A(q^2) - A_{\pi loop}(q^2) \right]. \quad (3)$$

To apply equation (3), we need experimental values for  $A(q^2)$  and  $F_\pi(q^2)$ . For the former, we use data from Brookhaven E865 [3]. Their amplitude  $f(q^2)$  is related to our  $A(q^2)$  by

$$|A(q^2)| = f(q^2) \frac{G_F \alpha}{4\pi} \quad (4)$$

where  $G_F$  is the Fermi constant and  $\alpha$  is the fine structure constant.

The experimental values of  $F_\pi$  from [1] are not in general at precisely the required values of  $q^2$ . However, the data, which are plotted in figure 2, are well described by the VMD model using a rho-meson pole:

$$F_\pi(q^2)_{VMD} = \frac{m_\rho^2}{m_\rho^2 - q^2} \quad (5)$$

for the region of  $q^2$  of interest. This is shown by the solid line in figure 2. Therefore we use equation (5) to calculate the required values of  $F_\pi$ . We emphasise that the values we calculate this way are essentially experimental; the VMD prediction is used basically as an interpolating function between the measured experimental points.

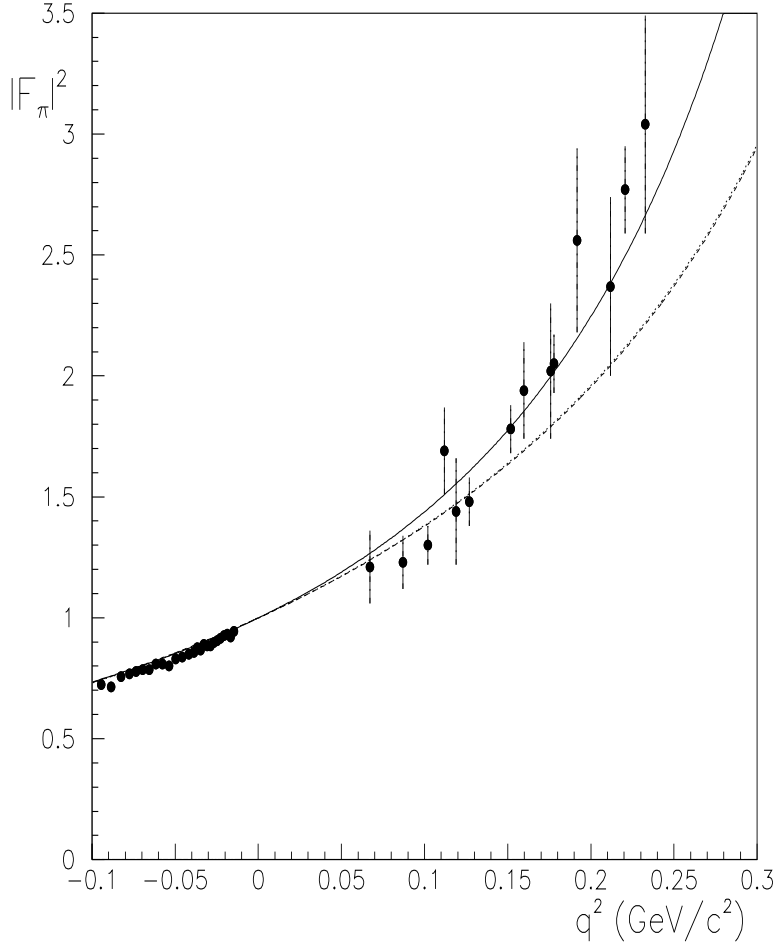


Figure 2: Pion electromagnetic form factors squared. The points are the experimental data. The curves are for VMD (solid line),  $L\sigma M$  (dashed line) and QT (dotted line). The dashed and dotted lines are practically indistinguishable in the figure.

The relative sign of  $A_{LD}$  and  $A_{\pi loop}$  was already established in [3] and [8]. To derive  $F_K$  from equation (3), we need also to determine the sign of  $F_K - F_\pi$ . To do so, we observe that in all models discussed below, as well as in the available data for  $q^2 < 0$ ,  $F_K$  differs less from unity than does  $F_\pi$ , i.e.

$$|F_K - 1| < |F_\pi - 1|.$$

This defines the required sign, giving

$$F_K = F_\pi - \frac{q^2(m_{K^+}^2 - m_{\pi^+}^2)}{e^2 |\langle \pi^+ | H_W | K^+ \rangle|} [A(q^2) - A_{\pi loop}(q^2)]. \quad (6)$$

The extracted values of  $|F_K|^2$  are listed in table 1 and plotted in figure 3 which also shows previous data for  $q^2 < 0$ . The errors in our values of  $F_K$  arise from experimental errors in the

Table 1: Experimental values for the kaon form factor from the present analysis.

$q^2$ (GeV/c) <sup>2</sup>	$ F_K(q^2) ^2$	$q^2$ (GeV/c) <sup>2</sup>	$ F_K(q^2) ^2$
0.0244	1.071 ± 0.083	0.0744	1.242 ± 0.082
0.0294	1.086 ± 0.083	0.0794	1.257 ± 0.082
0.0344	1.102 ± 0.083	0.0844	1.280 ± 0.081
0.0394	1.118 ± 0.083	0.0894	1.300 ± 0.081
0.0444	1.134 ± 0.083	0.0944	1.316 ± 0.081
0.0494	1.150 ± 0.082	0.0994	1.344 ± 0.081
0.0544	1.169 ± 0.082	0.1044	1.364 ± 0.081
0.0594	1.187 ± 0.082	0.1094	1.396 ± 0.081
0.0644	1.204 ± 0.082	0.1144	1.413 ± 0.081
0.0694	1.222 ± 0.082	0.1194	1.431 ± 0.082

amplitude  $A(q^2)$  for  $K^+ \rightarrow \pi^+ e^+ e^-$  and the error in the weak matrix element  $\langle \pi^+ | H_W | K^+ \rangle$ , but predominantly from the errors on the experimental values of  $F_\pi$ . The VMD model, equation (5), gives a reasonably unambiguous value for  $F_\pi$ . However, its use is only justified to the extent that it agrees with the experimental points in figure 2. The weighted RMS deviation of the positive- $q^2$  experimental points in figure 2 from the VMD prediction is 0.0837, and we take this as the error in  $|F_\pi|^2$ .

### 3. The Linear $\sigma$ Model

The quark-level Linear  $\sigma$  Model (L $\sigma$ M) has been discussed in several papers (e.g. [4, 5, 6, 12, 13]). Scadron *et al.*[5] gives the L $\sigma$ M expressions for meson form factors in the chiral limit (CL),

$$F(q^2)_{L\sigma M}^{CL} = -4ig^2 N_c / (16\pi^4) \int_0^1 dx \int d^4p [p^2 - m^2 + x(1-x)q^2]^{-2}. \quad (7)$$

Here,  $N_c$ , the number of colours, is related to the meson-quark coupling,  $g$ , by [5, 12]

$$g = 2\pi / \sqrt{N_c}. \quad (8)$$

Thus equation (7) becomes

$$F(q^2)_{L\sigma M}^{CL} = \frac{-i}{\pi^2} \int_0^1 dx \int d^4p [p^2 - m^2 + x(1-x)q^2]^{-2}. \quad (9)$$

In equations (7) and (9), setting  $m$  equal to the mean up-down constituent quark mass,  $\hat{m} = (m_u + m_d)/2$  gives the pion form factor,  $F_\pi$ . For the kaon form factor,  $m$  is set to the mean of  $\hat{m}$

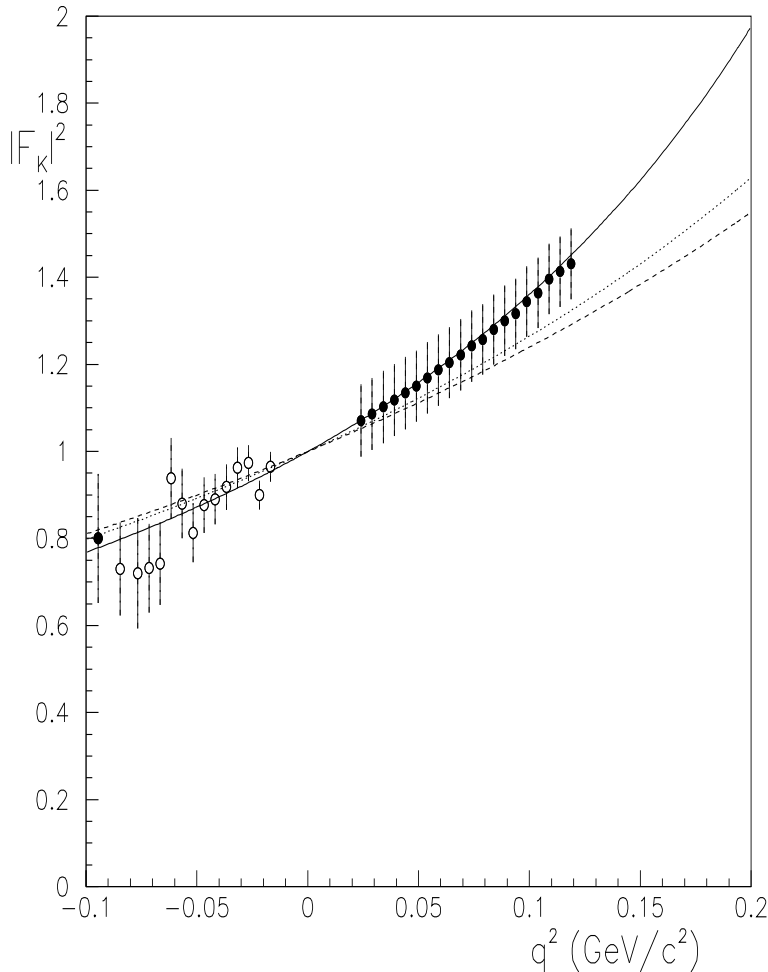


Figure 3: Kaon electromagnetic form factors squared. The solid points are the experimental data from the present analysis and the circles show the previously existing data. The curves are for VMD (solid line),  $L\sigma M$  (dashed line) and QT (dotted line).

and the s quark mass,  $m_{us} = (m_s + \hat{m})/2$ . In the present paper we use values in the chiral limit [14]:

$$\hat{m}^{CL} = 325.7 \text{ MeV}, \quad m_s^{CL} = 469.0 \text{ MeV}, \quad m_{us}^{CL} = 397.4 \text{ MeV}. \quad (10)$$

To avoid the divergence in equation (9), we use a Taylor-series expansion as follows. Differentiating equation (9) gives

$$\frac{dF(q^2)_{L\sigma M}^{CL}}{dq^2} = \frac{2i}{\pi^2} \int_0^1 dx \int \frac{d^4p}{[p^2 - m^2 + x(1-x)q^2]^3}. \quad (11)$$

The second integral in equation (11) can be written

$$I \equiv \int \frac{d^4 p}{[p^2 - V]^3} \quad (12)$$

where  $V = m^2 - x(1-x)q^2$ . Applying the Wick rotation,  $k^2 = -p^2$ ,  $d^4 p = i\pi^2 k^2 dk^2$ , this becomes

$$I = \int \frac{i\pi^2 k^2 dk^2}{[-k^2 - V]^3} \quad (13)$$

which can be integrated directly to give

$$I = -\frac{i\pi^2}{2V} \quad (14)$$

and hence, from equation (11),

$$\frac{dF(q^2)_{L\sigma M}^{CL}}{dq^2} = \int_0^1 \frac{x(1-x)}{V} dx. \quad (15)$$

As a check, the integral in equation (12) can be evaluated from the expression given by Scadron [16], and also by integration of the Taylor series for the charge radius given in [8].

At  $q^2 = 0$ ,  $V = m^2$  gives

$$\left[ \frac{dF(q^2)_{L\sigma M}^{CL}}{dq^2} \right]_{q^2=0} = \frac{1}{m^2} \int_0^1 x(1-x) dx = \frac{1}{6m^2}. \quad (16)$$

Further derivatives follow from differentiating equation (15). In writing a Taylor series for  $F(q^2)$ , the first term,  $F(0)_{L\sigma M}^{CL}$ , is given directly by the normalisation requirement that  $F(q^2) = 1$  at  $q^2 = 0$ . The series, therefore, is

$$F(q^2)_{L\sigma M}^{CL} = 1 + \frac{1}{6} \left( \frac{q}{m} \right)^2 + \frac{1}{60} \left( \frac{q}{m} \right)^4 + \frac{1}{420} \left( \frac{q}{m} \right)^6 + \frac{1}{2520} \left( \frac{q}{m} \right)^8 + \frac{1}{13860} \left( \frac{q}{m} \right)^{10} + \dots \quad (17)$$

As in equation (9), this series gives  $F_\pi(q^2)$  with  $m = \hat{m}$  and  $F_K(q^2)$  with  $m = m_{us}$ .

The form factors  $F_\pi(q^2)_{L\sigma M}^{CL}$  and  $F_K(q^2)_{L\sigma M}^{CL}$  predicted by equation (17) are plotted in figures 2 and 3, together with the data from the present analysis and from [1]. For both  $F_\pi(q^2)_{L\sigma M}^{CL}$  and  $F_K(q^2)_{L\sigma M}^{CL}$ , the L $\sigma$ M shows the same qualitative trend as the data, but falls somewhat below the experimental points.

#### 4. Quark triangle graphs

Scadron *et al* [5] describe another approach to meson form factors, *via* the quark-triangle graphs of figure 4. From [5], the pion and kaon form factors are given by

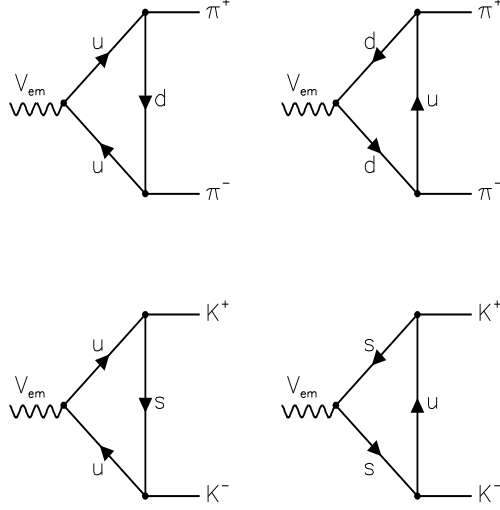


Figure 4: Quark-triangle graphs.

$$F_{\pi}(q^2)_{QT} = -4ig^2 N_c \left[ \frac{2}{3} I(q^2, m_u^2, m_d^2, m_{\pi}^2) + \frac{1}{3} I(q^2, m_d^2, m_u^2, m_{\pi}^2) \right], \quad (18)$$

$$F_K(q^2)_{QT} = -4ig^2 N_c \left[ \frac{2}{3} I(q^2, m_u^2, m_s^2, m_K^2) + \frac{1}{3} I(q^2, m_s^2, m_u^2, m_K^2) \right], \quad (19)$$

where

$$I(q^2, m_1^2, m_2^2, M^2) = \frac{i\pi^2}{2(2\pi)^4} \int_0^1 dv \int_v^1 du \frac{q^2 u + 2(M^2 - (m_1 - m_2)^2)(1 - u)}{m_2^2 - (M^2 + m_2^2 - m_1^2)u + M^2 u^2 + (v^2 - u^2)q^2/4} + \int_0^1 dx \int d^4 p \left[ p^2 - m_2^2 + (M^2 + m_2^2 - m_1^2)x - M^2 x^2 \right]^{-2}. \quad (20)$$

Here, we replace  $m_u$  and  $m_d$  by  $\hat{m}$  from equation (10). These expressions can be calculated either by direct evaluation of the integral in equation (20) or, as a check, by construction of a Taylor series by repeated differentiation of equation (20).

The results for the pion and kaon form factors are shown in figures 2 and 3. As for the L $\sigma$ M, the predictions for both  $F_K$  and  $F_{\pi}$  follow the data qualitatively, but detailed quantitative agreement is lacking.

## 5. Vector meson dominance

Finally, we examine a simple model based on VMD. As discussed in Sect. 2 above, the pion form factor is dominated in this model by the  $\rho$  pole, equation (5), and figure 2 shows that this simple picture agrees well with the data.

For the kaon form factor, there are contributions from the  $\rho$ ,  $\omega$  and  $\phi$  poles:

$$F_K(q^2)_{VMD} = N \left( \frac{1}{2} \frac{g_{\rho ee}}{m_{\rho^0}^2 - q^2} + \frac{1}{2} \frac{g_{\omega ee}}{m_{\omega}^2 - q^2} + \sqrt{\frac{1}{2}} \frac{g_{\phi ee}}{m_{\phi}^2 - q^2} \right). \quad (21)$$

where  $g_{\rho ee} = 4.97$ ,  $g_{\omega ee} = 17.06$  and  $g_{\phi ee} = 13.38$ , derived from the decay widths. The  $\rho^0 K^+ K^-$ ,  $\omega K^+ K^-$  and  $\phi K^+ K^-$  SU(3) coefficients are  $\frac{1}{2}$ ,  $\frac{1}{2}$  and  $\frac{1}{\sqrt{2}}$  respectively. The requirement that  $F(0) = 1$  gives the normalisation coefficient as  $N = 0.03682 \text{ GeV}^2$ .

The prediction of equation (21) is plotted with the data for  $F_K$  in figure 3. As for  $F_{\pi}$ , the VMD gives excellent agreement with data, both for the previously available data for  $q^2 < 0$  and for the new data derived in the present paper.

## 6. Slopes of form factors at $q^2 = 0$ .

In this section we examine two properties that depend on the slopes of the form factors at  $q^2 = 0$ , i.e. the meson charge radii and the amplitude for  $K^+ \rightarrow \pi^+ e^+ e^-$  at  $q^2 = 0$ . Predictions for charge radii have been published before [5] but we include them here for completeness and because we update some numerical values.

The charge radius is related to the form factor by [5]

$$r \equiv \sqrt{\langle r^2 \rangle} = \sqrt{6 \left[ \frac{dF(q^2)}{dq^2} \right]_{q^2=0}}. \quad (22)$$

For the L $\sigma$ M and VMD, the quantity  $dF(q^2)/dq^2$  is straightforwardly obtained from equations (16), (5) and (21). For the QT model, the expression is given by [5] as

$$\langle r_{\pi}^2 \rangle = \frac{g^2 N_c}{4\pi^2 \hat{m}^2} = \left[ \frac{\hbar c}{\hat{m}} \right]^2 \quad (23)$$

and

$$\langle r_K^2 \rangle = \frac{g^2 N_c}{4\pi^2 \hat{m}^2} \left( 1 - \frac{5}{6} \delta + \frac{3}{5} \delta^2 - \frac{4}{9} \delta^3 + \frac{22}{63} \delta^4 - \frac{2}{7} \delta^5 + \dots \right). \quad (24)$$

where  $\delta = (m_s/\hat{m}) - 1 = 0.44$  (see also [17]).

The predictions are compared with the experimental values from [2] in table 2.

Table 2: Meson charge radii and amplitudes for  $K^+ \rightarrow \pi^+ e^+ e^-$  at  $q^2 = 0$ .

Model	$r_\pi$ (fm)	$r_K$ (fm)	$A(0)$ $10^{-9} \text{ GeV}^{-2}$
L $\sigma$ M	0.606	0.497	7.56
QT	0.606	0.514	6.47
VMD	0.623	0.574	3.69
Experiment	$0.672 \pm 0.008$	$0.56 \pm 0.03$	$4.00 \pm 0.18$

The LD contribution to the amplitude for  $K^+ \rightarrow \pi^+ e^+ e^-$  at  $q^2 = 0$  is given by equation (1) as

$$|A_{LD}(0)| = e^2 \left| \frac{\langle \pi^+ | H_W | K^+ \rangle}{m_{K^+}^2 - m_{\pi^+}^2} \right| \left| \frac{dF_{\pi^+}}{dq^2} - \frac{dF_{K^+}}{dq^2} \right|_{q^2=0}. \quad (25)$$

Since the pion loop term vanishes at  $q^2 = 0$ , equation (25) gives the total amplitude directly. For the three models considered here,  $A(0)$  can be calculated using the expressions for the derivatives given above. We take the experimental value from Brookhaven E865 [3], converting their  $f_0$  to our  $A(0)$  using equation (4).

From table 2, we see that the VMD picture again comes closest to a quantitative description of the data. As expected, this is consistent with the conclusion from the form factors of figures 2 and 3.

## 7. Summary

We have derived new experimental values for  $F_K$  for positive  $q^2$  from the decay  $K^+ \rightarrow \pi^+ e^+ e^-$ , extending the range over which experimental values of  $F_K(q^2)$  are known to  $-0.1 (\text{GeV}/c)^2 < q^2 < 0.125 (\text{GeV}/c)^2$ . Also, we have calculated both  $F_\pi$  and  $F_K$  for the range of  $q^2$  covered by these new data and the previous data, and have examined the slopes at  $q^2 = 0$ . It is apparent that for all these comparisons, the L $\sigma$ M and the QT model give at best a qualitative description of the data, while the VMD model gives a detailed quantitative fit.

## Acknowledgments

We acknowledge support from the US DOE.

## References

- [1] Bereshnev S F *et al* 1974 *Sov. J. Nucl. Phys.* **18** 53  
 Bereshnev S F *et al* 1976 *Sov. J. Nucl. Phys.* **24** 591  
 Quezner A *et al* 1978 *Phys. Lett. B* **76** 512  
 Vasserman I B *et al* 1981 *Sov. J. Nucl. Phys.* **33** 368

Amendolia S R *et al* 1985 *Phys. Lett. B* **138** 454

Barkov L M *et al* 1985 *Nucl. Phys. B* **256** 365

Amendolia S R *et al* 1986 *Phys. Lett. B* **178** 435

Amendolia S R *et al* 1986 *Nucl. Phys. B* **277** 168

The last of these references contains an excellent summary of all earlier work.

[2] Particle Data Group, Eidelman S *et al* 2004 *Phys. Lett. B* **592** 1

[3] Appel R *et al* 1999 (E865 collaboration) *Phys. Rev. Lett.* **83** 4482

[4] Gell-Mann M and Levy M 1960 *Nuovo Cim.* **16** 705

[5] Scadron M D, Kleefeld F, Rupp G and van Beveren E 2003 *Nucl. Phys. A* **724** 391 (hep-ph/0211275)

[6] Scadron M D, Rupp G, Kleefeld F and van Beveren E 2004 *Phys. Rev. D* **69** 014010 (hep-ph/0309109)

[7] Eilam G and Scadron M D 1985 *Phys. Rev. D* **31** 2263

[8] Burkhardt H *et al* 2001 *Phys. Lett. B* **512** 317 (hep-ph/0011345)

[9] Dib C O, Dunietz I and Gilman F J 1989 *Phys. Rev. D* **39** 2639

[10] Ecker G, Pich A and deRafael E 1987 *Nucl. Phys. B* **291** 692

D'Ambrosio G, Ecker G, Isidori G and Portolés J 1998 *JHEP* **8** 4

[11] Lowe J and Scadron M D 2002 *Mod. Phys. Lett. A* **17** 2497 (hep-ph/0208118)

[12] Delbourgo R and Scadron M D 1995 *Mod. Phys. Lett. A* **10** 251

[13] Paver N and Scadron M D 1983 *Nuovo Cim. A* **78** 159

Elias V and Scadron M D 1984 *Phys. Rev. Lett.* **53** 1129

[14] We derive values for the quark masses in the chiral limit as follows. The Goldberger-Treiman relation [5, 15]  $\hat{m}^{CL} = f_{\pi}^{CL} g = 325.7$  MeV for  $g = 2\pi/\sqrt{3}$  from reference 14 of [15] due to the once-subtracted dispersion relation for  $f_{\pi}$  (see equation (19) of [15]). Also [2, 5, 15],  $m_s/\hat{m} = 2f_K/f_{\pi} - 1 = 1.44$  so that  $m_s^{CL} = 469.0$  MeV.

[15] Nagy M, Scadron M D and Hite G E 2004 *Acta Physica Slovaca* **54** 427 (hep-ph/0406009)

[16] Scadron M D 1990 *Advanced Quantum Theory* (Berlin: Springer-Verlag) p 392

[17] Ayala C and Bramon A 1987 *Europhys. Lett.* **4** 777